Application of Sphere Decoding in Intercarrier-Interference Reduction for OFDM Systems

Y. J. Kou, W.-S. Lu, and A. Antoniou
Department of Electrical and Computer Engineering, University of Victoria
P.O. Box 3055, Victoria, B.C., Canada V8W 3P6
Email: {ykou, wslu}@ece.uvic.ca, aantoniou@ieee.org

***Abstract*— While fast variations of wireless channel characteristics cause intercarrier interference (ICI) in orthogonal frequency-division multiplexing systems, they also introduce frequency diversity, which can be exploited to improve the demodulation performance. An ICI-reduction algorithm is proposed based on a sphere decoding (SD) algorithm. By considering channel information, a new search strategy is developed to reduce the computational complexity of the SD algorithm. Design examples are presented which demonstrate that the proposed algorithm outperforms several existing algorithms in terms of BER performance.**

I. Introduction

Orthogonal frequency-division multiplexing (OFDM) has recently been used for data transmission in a number of communication systems [1]-[2]. Unfortunately, there are several drawbacks associated with OFDM modulation. In a rapidly fading environment, channel variations within an OFDM symbol duration lead to a loss of orthogonality in the OFDM subcarrier waveforms and result in intercarrier interference (ICI) which, in turn, degrades the bit-error-rate (BER) performance of the system [3]. If not compensated for, ICI will result in an error floor that increases with Doppler frequency. However, channel variations also introduce frequency diversity which can be exploited to improve system performance [4]. Recently, a number of algorithms have been proposed to mitigate the effect of ICI [5]-[6]. In [5], a linear minimum mean-square error (MMSE) has been proposed. Since the number of subcarriers is generally quite large, this algorithm requires intensive computation. In attempts to reduce the computational complexity, a decision feedback (DF) algorithm has been derived in [6] where only signals on several neighbouring subcarriers are used in order to suppress the ICI for a particular subcarrier. The computational complexity of this algorithm is reduced at the cost of a slight degradation of performance.

In this paper, an ICI-reduction algorithm based on the sphere decoding (SD) algorithm [7] is proposed. By considering channel information, a new search strategy for the reduction of the compelxity of the SD algorithm is developed. It is demonstrated by simulations that the proposed algorithm outperforms several existing algorithms in terms of BER performance. It is also shown that, because of the frequency diversity introduced by channel variations, improved performance can be achieved by the proposed algorithm at higher Doppler frequencies.

II. Signal Model

Consider an N-subcarrier OFDM transmitter as illustrated in Fig. 1, where S/P, P/S, and DAC represent serial-to-parallel, parallel-to-serial, and digital-to-analog converters, respectively, and the block labeled as "Amp." represents a power amplifier (PA). The information bits D_k and the modulated symbol X_k are referred to as the *data point* and *subsymbol* at the kth subcarrier, respectively. Vectors $\mathbf{X} = [X_0, \ldots, X_{N-1}]^T$ and $\mathbf{x} = [x_0, \ldots, x_{N-1}]^T$ are referred to as the frequency-domain and the time-domain $OFDM\ symbol$s, respectively.

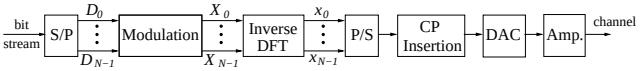

Fig. 1. An OFDM transmitter.

Mathmetically, the OFDM symbol $\mathbf{x}$ can be obtained by using the inverse discrete Fourier transform (IDFT) as

$$x_n = \frac{1}{N}\sum_{k=0}^{N-1} X_k e^{j2\pi kn/N} \qquad \text{for } n = 0, \ldots, N-1 \tag{1}$$

where x_n represents the nth element of $\mathbf{x}$. In matrix form, (1) can be expressed as

$$\mathbf{x} = \mathbf{Q}\mathbf{X} \tag{2}$$

where $\mathbf{Q}$ is the IDFT matrix whose elements are $q_{n,k} = (1/N)e^{j2\pi kn/N}$. A cyclic prefix (CP) with length equal to that of the channel impulse response (CIR) is inserted in the beginning of the OFDM symbol before it is transmitted into the channel. Denoting the transmitted and received signals as $\mathbf{x}_{CP} = [x_{N-L+1}, \ldots, x_{N-1}, x_0, \ldots, x_{N-1}]^T$ and $\mathbf{y} = [y_0, \ldots, y_{N-1}]^T$, respectively, the received signal can be written as

$$\mathbf{y} = \mathbf{H}_{CP}\mathbf{x}_{CP} + \mathbf{n} \tag{3}$$

where $\mathbf{n} = [n_0, \ldots, n_{N-1}]^T$ is a vector of additive white Guassian noise (AWGN) variables with zero mean and covariance matrix $\mathcal{E}\left[\mathbf{n}\mathbf{n}^H\right] = \sigma^2\mathbf{I}$, and the channel matrix $\mathbf{H}_{CP}$ is given by

$$\mathbf{H}_{CP} = \begin{bmatrix} h_0^{L-1} & h_0^{L-2} & \cdots & h_0^0 & 0 & \cdots & 0 & 0 \\ 0 & h_1^{L-1} & \cdots & h_1^1 & h_1^0 & \cdots & 0 & 0 \\ \vdots & \vdots & \ddots & \vdots & \vdots & \ddots & \vdots & \vdots \\ 0 & 0 & \cdots & 0 & 0 & \cdots & h_{N-1}^1 & h_{N-1}^0 \end{bmatrix} \tag{4}$$

where h_n^l for $n = 0, \ldots, N-1$ and $l = 1, \ldots, l$ represents the fading coefficient of the lth path at the nth sample instance. Since the CP is only a copy of part of the OFDM symbol $\mathbf{x}$, (3) can be rewritten as

$$\mathbf{y} = \mathbf{H}\mathbf{x} + \mathbf{n} \tag{5a}$$

where

$$\mathbf{H} = \begin{bmatrix} h_0^0 & 0 & \cdots & h_0^2 & h_0^1 \\ h_1^1 & h_1^0 & \cdots & h_1^3 & h_1^2 \\ \vdots & \vdots & \ddots & \vdots & \vdots \\ h_{L-1}^{L-1} & h_{L-1}^{L-2} & \cdots & 0 & 0 \\ \vdots & \vdots & \ddots & \vdots & \vdots \\ 0 & 0 & \cdots & h_{N-2}^0 & 0 \\ 0 & 0 & \cdots & h_{N-1}^1 & h_{N-1}^0 \end{bmatrix} \tag{5b}$$

At the receiver, after the removal of the CP, the received signal is transformed to $\mathbf{Y} = [Y_0, \ldots, Y_{N-1}]^T$ by using the discrete Fourier transform (DFT) as

$$\mathbf{Y} = \mathbf{Q}^H \mathbf{y} \tag{6}$$

From (2), (5a), and (6), $\mathbf{Y}$ can be expressed as

$$\mathbf{Y} = \mathbf{A}\mathbf{X} + \mathbf{N} \tag{7a}$$

where

$$\mathbf{A} = \mathbf{Q}^H \mathbf{H} \mathbf{Q} \tag{7b}$$

and $\mathbf{N} = [N_0, \ldots, N_{N-1}]^T = \mathbf{Q}^H \mathbf{n}$. Since the DFT matrix $\mathbf{Q}^H$ is unitary, $\mathbf{N}$ in (7a) is still white Guassian noise. Due to channel variations, matrix $\mathbf{A}$ is not a diagonal matrix. Therefore, the received signal at any subcarrier depends not only on the transmitted signal at that subcarrier but also on the transmitted signals at other subcarriers, where the latter are the ICI caused by channel variations. In order to mitigate the effect of the ICI, joint detection (JD) is required at the receiver. A general structure for the OFDM receiver that implements a JD algorithm is illustrated in Fig. 2. For the signal detection problem in (7), maximum likelihood (ML) detection [8] can be carried out by solving the optimization problem

$$\text{minimize} \quad \|\mathbf{Y} - \mathbf{A}\mathbf{X}\|_2^2 \tag{8a}$$

$$\text{subject to :} \quad X_k \in \mathcal{M} \quad \text{for } k = 0,\ 1,\ \ldots,\ N-1 \tag{8b}$$

where $\mathcal{M}$ is the set of the constellation points associated with the modulation scheme of the OFDM system. In what follows, an SD algorithm is proposed which can be used to solve the optimization problem in (8).

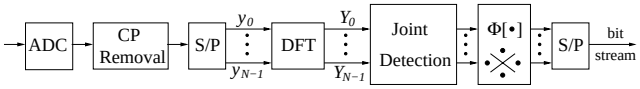

Fig. 2. An OFDM receiver.

III. A Sphere Decoding Algorithm for ICI Reduction

The variables in (8) are complex-valued. If we let $\mathbf{Y} = \mathbf{Y}_r + j\mathbf{Y}_i$, $\mathbf{A} = \mathbf{A}_r + j\mathbf{A}_i$, and $\mathbf{X} = \mathbf{X}_r + j\mathbf{X}_i$, then the norm in (8a) assumes the form

$$\|\tilde{\mathbf{Y}} - \tilde{\mathbf{A}}\tilde{\mathbf{X}}\|_2^2 \tag{9a}$$

where

$$\tilde{\mathbf{Y}} = \begin{bmatrix} \mathbf{Y}_r \\ \mathbf{Y}_i \end{bmatrix}, \tilde{\mathbf{A}} = \begin{bmatrix} \mathbf{A}_r & -\mathbf{A}_i \\ \mathbf{A}_i & \mathbf{A}_r \end{bmatrix}, \tilde{\mathbf{X}} = \begin{bmatrix} \mathbf{X}_r \\ \mathbf{X}_i \end{bmatrix} \tag{9b}$$

and the problem in (8) can be expressed as

$$\text{minimize} \quad \|\tilde{\mathbf{Y}} - \tilde{\mathbf{A}}\tilde{\mathbf{X}}\|_2^2 \tag{10a}$$

$$\text{subject to :} \quad \tilde{X}(i) \in \tilde{\mathcal{M}} \quad \text{for } i = 0,\ 1,\ \ldots,\ 2N-1 \tag{10b}$$

where $\tilde{\mathcal{M}}$ represents the set of points associated with the real and imaginary components of the modulation constellation. For the sake of simplicity, 4-QAM modulation is assumed for all subcarriers and, therefore, we have $\tilde{\mathcal{M}} = \{1, -1\}$. In an attempt to improve the performance, vector $\tilde{\mathbf{X}}$ is re-ordered according to the asymptotic effective energy of each element [9] and the columns of matrix $\tilde{\mathbf{A}}$ are re-ordered accordingly. Let $\mathbf{s} = \text{order}(\tilde{\mathbf{X}})$ and $\mathbf{G} = \text{order}(\tilde{\mathbf{A}})$ represent the re-ordered vector $\tilde{\mathbf{X}}$ and matrix $\tilde{\mathbf{A}}$, respectively. The objective function in (10a) becomes $\|\tilde{\mathbf{Y}} - \mathbf{G}\mathbf{s}\|_2^2$ and the problem in (10) can be rewritten as

$$\text{minimize} \quad \|\tilde{\mathbf{Y}} - \mathbf{G}\mathbf{s}\|_2^2 \tag{11a}$$

$$\text{subject to :} \quad s_i \in \{1, -1\} \quad \text{for } i = 0,\ 1,\ \ldots,\ 2N-1 \tag{11b}$$

where s_i represents the ith element of vector $\mathbf{s}$. By using the QR-decomposition, matrix $\mathbf{G}$ can be expressed as

$$\mathbf{G} = \mathbf{Q}\mathbf{R} \tag{12}$$

where $\mathbf{Q}$ and $\mathbf{R}$ are orthogonal and upper triangular matrices, respectively. If we let $\mathbf{p} = \mathbf{Q}^T\tilde{\mathbf{Y}}$, the objective function in (11a) can be obtained as

$$\|\tilde{\mathbf{Y}} - \mathbf{G}\mathbf{s}\|_2^2 = \|\mathbf{p} - \mathbf{R}\mathbf{s}\|_2^2 \tag{13}$$

and the problem in (11) becomes

$$\text{minimize} \quad \|\mathbf{p} - \mathbf{R}\mathbf{s}\|_2^2 \tag{14a}$$

$$\text{subject to :} \quad s_i \in \{1, -1\} \quad \text{for } i = 0,\ 1,\ \ldots,\ 2N-1 \tag{14b}$$

The solution of the problem in (14) can be obtained by applying an SD algorithm [7] that takes into account the special structure of $\mathbf{R}$. The basic idea of an SD algorithm is to search only lattice points that lie in a certain hypersphere of radius r around the given vector $\mathbf{p}$ and therefore the search space is reduced compared with that of the exhaustive search algorithms. Note that a necessary and sufficient condition for a point $\mathbf{R}\mathbf{s}$ to lie within the hypersphere of radius $r = r_{2N-1}$ is that the modulus of distance vector between the point $\mathbf{R}\mathbf{s}$ and the center point $\mathbf{p}$ is less than the radius, namely,

$$\|\mathbf{p} - \mathbf{R}\mathbf{s}\|_2^2 \le r_{2N-1}^2 \tag{15a}$$

which can also be written as

$$\sum_{i=0}^{2N-1} \left(p_i - \sum_{j=i}^{2N-1} R_{ij} s_j \right)^2 \le r_{2N-1}^2 \tag{15b}$$

where p_i and R_{ij} represent the ith element of $\mathbf{p}$ and the (i,j)th element of $\mathbf{R}$, respectively. The left-hand side (l.h.s.) of (15b) can be expanded as

$$\begin{aligned}(p_{2N-1} - R_{2N-1,2N-1}s_{2N-1})^2 + (p_{2N-2} - R_{2N-2,2N-1}s_{2N-1} \\ - R_{2N-2,2N-2}s_{2N-2})^2 + \ldots \le r_{2N-1}^2\end{aligned} \tag{16}$$

By considering only the first term on the l.h.s. of (16), a necessary condition for $\mathbf{R}\mathbf{s}$ to lie within the hypersphere can be obtained as

$$(p_{2N-1} - R_{2N-1,2N-1}s_{2N-1})^2 \le r_{2N-1}^2 \tag{17}$$

and the feasible region for s_{2N-1} is given by

$$\left\lceil \frac{-r_{2N-1} + p_{2N-1}}{R_{2N-1,2N-1}} \right\rceil \le s_{2N-1} \le \left\lfloor \frac{r_{2N-1} + p_{2N-1}}{R_{2N-1,2N-1}} \right\rfloor \tag{18}$$

where $\lceil \cdot \rceil$ and $\lfloor \cdot \rfloor$ represent the ceiling and floor functions, respectively. By considering the first two terms on the l.h.s. of (16), an improved necessary condition can be obtained as

$$(p_{2N-2,2N-1} - R_{2N-2,2N-2}s_{2N-2})^2 \le r_{2N-2}^2 \tag{19a}$$

where

$$\begin{aligned} r_{2N-2}^2 &= r_{2N-1}^2 - (p_{2N-1} - R_{2N-1,2N-1}s_{2N-1})^2 \\ p_{2N-2,2N-1} &= p_{2N-1} - R_{2N-2,2N-1}s_{2N-1} \end{aligned} \tag{19b}$$

Thus, the feasible region of s_{2N-2} can be obtained as

$$\left\lceil \frac{-r_{2N-2}+p_{2N-2,2N-1}}{R_{2N-2,2N-2}} \right\rceil \le s_{2N-2} \le \left\lfloor \frac{r_{2N-2}+p_{2N-2,2N-1}}{R_{2N-2,2N-2}} \right\rfloor$$

In a similar fashion, the remaining elements of $\mathbf{s}$ can be obtained successively as

$$\left\lceil \frac{-r_k+p_{k,k+1}}{R_{k,k}} \right\rceil \le s_k \le \left\lfloor \frac{r_k+p_{k,k+1}}{R_{k,k}} \right\rfloor \tag{20a}$$

where

$$\begin{aligned} r_k^2 &= r_{k+1}^2-(p_{k+1}-R_{k+1,k+1}s_{k+1})^2 \\ p_{k,k+1} &= p_{k+1}-R_{k,k+1}s_{k+1} \end{aligned} \tag{20b}$$

for $k=2N-3,\ldots,1$. Based on the feasible region of s_k in (20), one can determine the value of s_k accordingly. It can be observed that the above procedure actually constructs a binary tree as illustrated in Fig. 3, where the branches at the kth level of the tree represent the values of the kth component of vector $\mathbf{s}$. Each path from top to bottom, i.e., level $2N-1$ to level 0, represents a vector $\mathbf{s}$ so that point $\mathbf{Rs}$ lies in the hypersphere. By using the above procedure, all lattice points in the hypersphere can be determined and the solution of the problem in (14) can be obtained by finding the path such that the distance between the corresponding point and the center point is minimized.

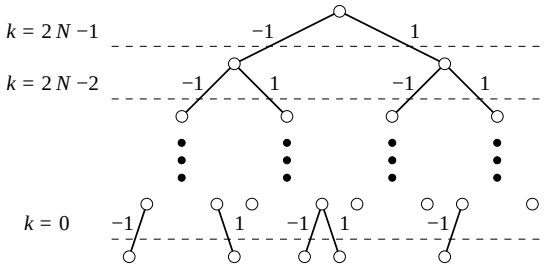

Fig. 3. A binary tree constructed for the search of lattice points in a $2N$-dimensional hypersphere.

The value of the initial radius of the $2N$-dimensional hypersphere can be chosen as infinity. Thus, it is guranteed that a point inside the hypersphere can be found. Once this is done, the radius of the hypersphere can be replaced by the distance between the newly found point and the center point. Since the radius of the hypersphere of interest reduces consistently as the algorithm proceeds, the initial setup of the radius does not increase the computational complexity of the algorithm.

In order to explain the tree search process, a flag is established at each level to indicate the status of the branches, i.e., $\{b_k = [b_k(1)\ b_k(2)]^T\colon k=2N-1,\ldots,0\}$ where $b_k(1)$ and $b_k(2)$ are used to indicate the status of the left and right branches at the kth level, respectively. For example, if $s_k=-1$ falls into the feasible region in (20a), then the left branch at the kth level is open and $b_k(1)=1$; otherwise, the left branch at the kth level is closed and $b_k(1)=0$.

At the beginning of the tree search, a depth-first search strategy can be used. At the kth branch level, flag b_k is obtained based on the feasible region given in (20) and s_k can be determined as follows. If $b_k(1)=b_k(2)=0$, then both branches are closed. As a result, no feasible solution of s_k is available, and the search reaches a dead end and stops at this level. If only one of the elements of b_k is equal to one, then there is only one open branch and s_k can be determined uniquely as the value corresponding to the open branch. If $b_k(1)=b_k(2)=1$, then both branches are open. In such a case, s_k can be obtained as the value that minimizes r_{k-1}, i.e.,

$$s_k = \arg\left(\min_{s_k\in\{-1,1\}} r_{k-1}\right) \tag{21}$$

When s_k is determined, the corresponding element of flag b_k is set to zero and the tree search enters into the $(k-1)$th level. The depth-first search continues until the first point inside the hypersphere is found as $\mathbf{s}_1$, and $\mathbf{s}_1$ is set to the current solution of the problem in (14). Denoting the path through which $\mathbf{s}_1$ is found as P^1, the radius of the hypersphere can be updated as $r_{2N-1}^1=\|\mathbf{p}-\mathbf{Rs}_1\|_2^2$, where the superscipt indicates the radius is updated using the information of path P^1. The feasible region of $\{s_k : k=2N-1,\ldots,0\}$ can be updated using (20) and the status of the branches can be updated accordingly as $\{b_k^1 : k=2N-1,\ldots,0\}$. In an attempt to avoid repetitions, the branches that have been visited in P^1 are kept closed. If there is no open branch at any level, then $\mathbf{s}_1$ is the exact solution of the problem in (14). Otherwise, the tree search needs to be continued.

In an attempt to improve the efficiency of the algorithm, a probabilistic search strategy is applied in the following search that maximizes the probability that the current feasible solution is optimal. It can be shown that if only one bit of vector $\mathbf{s}$ is detected incorrectly, then the probability that the detection error occurs in s_k is inversely related to the absolute value of $R_{k,k}$. Let the elements on the main diagonal of $\mathbf{R}$ be ordered from smallest to largest according to their absolute values. The open branch in P^1 at the level with the smallest absolute value of $R_{k,k}$ can be selected as the start point of the following search. Such a choice is guaranteed to maximize the probability that a one-bit detection error is corrected. When the start point of the following search is determined, the depth-first search strategy can be applied until a new point inside the hypersphere is found or a dead end is reached. If a new point inside the hypersphere is found as $\mathbf{S}_2$, then $\mathbf{s}_2$ is set to the current solution of the problem in (14) and this path is donoted as P^2. The radius of the hypersphere can be updated as $r_{2N-1}^2=\|\mathbf{p}-\mathbf{Rs}_2\|_2^2$. The status of the branches in paths P^1 and P^2 can be updated accordingly as $\{b_k^1 : k=2N-1,\ldots,0\}$ and $\{b_k^2 : k=2N-1,\ldots,0\}$, respectively. On the other hand, if a dead end is reached, then the path is denoted as a dead-end path P^2 and no further update is needed.

In the next round of the tree search, the open branch at the level with smallest absolute value of $R_{k,k}$ can be chosen as the start point. The search process continues until all the branches in all paths are closed, and, then the current solution of $\mathbf{s}$ is deemed to be the solution of the problem in (14). A stopping criterion can be established to reduce the complexity of the algorithm. For example, we count the number of dead-end branches that have been visited since the most recent point inside the hypersphere is found; if this number reaches a predefined threshold itr_{max} before a new point inside the hypersphere is found, then the algorithm stops and the current value of $\mathbf{s}$ is taken to be the solution of the problem in (14). A step-by-step description of the above SD algorithm is listed in Table 1.

IV. Simulations

The proposed ICI-reduction algorithm was applied to an OFDM system where the number of subcarriers was chosen to be 64 and 4-QAM was adopted as the modulation scheme for each subcarrier. The bandwidth of the OFDM system and the carrier frequency were set to $B=200$ kHz and $f_c=2$ GHz, respectively. The length of the CP was set to $N_pT_c=(N/8)T_c=T_s/8$, where T_s and T_c

TABLE I

A SPHERE DECODING ALGORITHM FOR ICI REDUCTION

Step 1

Input $\mathbf{Y}$, $\mathbf{A}$, $\mathbf{X}$, and itr_{max}.

Calculate $\mathbf{p}$ and $\mathbf{R}$ using (9)-(13).

Set $K = 1$ and the initial radius to infinity.

Apply the depth-first search.

Record the solution $\mathbf{s}_1$.

Update r_k^1 and b_k^1 for $k = 2N-1, \ldots, 0$.

Step 2

Set $itr = 0$.

Step 3

Set $K = K + 1$.

If no open branch is available, then go to **Step 4.**

Otherwise, find the start point using the probabilistic search strategy.

Apply the depth-first search.

If a new point inside the hypersphere is found, then update r_k^n and b_k^n for $k = 2N-1, \ldots, 0$ and $n = 1, \ldots, K$, and record the solution $\mathbf{s}_K$. Go to **Step 2.**

Otherwise, set $itr = itr + 1$.

If $itr > itr_{max}$, then go to **Step 4,**

Otherwise, go to **Step 3.**

Step 4

Output $\mathbf{s}_K$ as the solution of the problem in (14) and stop.

are the time durations of OFDM symbols and chips respectively. A two-tap Rayleigh fading channel model [6] was assumed where the Doppler frequency of the channel is denoted as f_D. While the delay of the first tap was zero, the delay of the second tap was randomly generated from $\{T_c, 2T_c, \ldots, N_pT_c\}$ with equal probability. The BER performance of the proposed algorithm was evaluated and compared with that of several existing algorithms under a variety of system configurations. For the DF algorithm in [6], the number of neighbouring subcarriers that were used to suppress the ICI at a particular subcarrier was taken to be $2K + 1$.

Example: For the proposed ICI-reduction algorithm, the BER versus the ratio of energy-per-bit to spectral noise density (Eb/N0) is plotted in Fig. 4 as solid and dash curves, respectively, for the cases of $f_DT_s = 0.1$ and $f_DT_s = 0.25$. For the sake of comparison, the BER of the DF algorithm in [6] is plotted in the same figure for various values of K as dotted curves. It can be observed that improved performance can be obtained by the proposed algorithm compared with that of the DF algorithm. For example, for the case of $f_DT_s = 0.1$ and at the BER level of 10^{-3}, a 3-dB and 1.5-dB improvement of Eb/N0 can be achieved by the proposed algorithm compared with the DF algorithm with $K = 5$ and $K = 15$, respectively. It can also be observed that the performance of the proposed algorithm improves with an increase in the Doppler frequency. For example, while for the case of $f_DT_s = 0.1$ an $Eb/N0 = 27$ dB is required to achieve the BER level of 10^{-3}, for the case of $f_DT_s = 0.25$ an $Eb/N0 = 24.5$ dB is required to achieve the same BER level. This improvement with increasing f_D can be attributed to the increase in frequency diversity introduced by the higher Doppler spread [4].

V. CONCLUSIONS

An ICI-reduction algorithm based on the sphere decoding algorithm has been proposed. Design examples have been presented which demonstrate that the proposed algorithm outperforms several existing algorithms in terms of bit-error-rate performance. It has also been shown that the proposed algorithm exploits the frequency diversity introduced by channel variations and, therefore, improved performance can be achieved at higher Doppler frequencies.

ACKNOWLEDGEMENT

The authors are grateful to Micronet, NCE Program, and the Natural Sciences and Engineering Research Council of Canada for supporting this work.

REFERENCES

[1] ETSI, "Digital video broadcasting: framing structure, channel coding, and modulation for digital terrestrial television," European Telecommunication Standard, ETS 300-744, Aug. 1997.

[2] IEEE 802.11, "IEEE Standard for Wireless LAN Medium Access Control (MAC) and Physical Layer (PHY) specifications," Nov. 1997.

[3] Y. Li and L. J. Cimini, Jr., "Bounds on the interchannel interference of OFDM in time-varying impairments," *IEEE Trans. Commun.*, vol. 49, pp. 401-404, Mar. 2001.

[4] N. J. Bass and D. P. Taylor "Matched filter bounds for wireless communication over Rayleigh fading dispersive channel," *IEEE Trans. Commun.*, vol. 49, pp. 1525-1528, Sep. 2001.

[5] Y.-S. Choi, P. J. Voltz, and F. A. Cassara "On channel estimation and detection for multicarrier signals in fast and selective Rayleigh fading channels," *IEEE Trans. Commun.*, vol. 49, pp. 1375-1387, Aug. 2001.

[6] X. Cai and G. B. Giannakis "Bounding performance and suppressing intercarrier interference in wireless mobile OFDM," *IEEE Trans. Commun.*, vol. 51, pp. 2047-2056, Dec. 2003.

[7] U. Fincke and M. Pohst, "Improved methods for calculating vectors of short length in a lattice, including a compelxity analysis" *Math. Comput.*, vol. 44, pp. 463-471, Apr. 1985.

[8] J. G. Proakis, *Digital Communications*, 4th ed., McGraw-Hill, 2000.

[9] M. Varanasi, "Decision feedback multiuser detection: A systematic approach," *IEEE Trans. Information Theory*, vol. 45, no. 1, pp. 219-240, Jan. 1999.

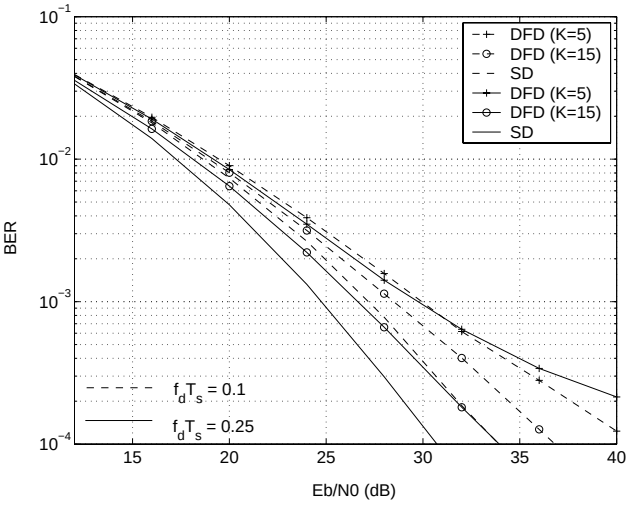

Fig. 4. Performance of ICI-reduction algorithms with various f_dT_s.